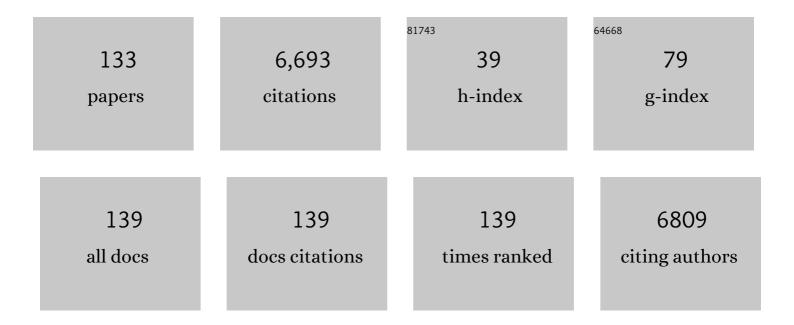
Werner Baumgartner

List of Publications by Year in descending order

Source: https://exaly.com/author-pdf/3908764/publications.pdf

Version: 2024-02-01



#	Article	IF	CITATIONS
1	Detection and localization of individual antibody-antigen recognition events by atomic force microscopy Proceedings of the National Academy of Sciences of the United States of America, 1996, 93, 3477-3481.	3.3	1,116
2	Imaging of single molecule diffusion Proceedings of the National Academy of Sciences of the United States of America, 1996, 93, 2926-2929.	3.3	593
3	Cadherin interaction probed by atomic force microscopy. Proceedings of the National Academy of Sciences of the United States of America, 2000, 97, 4005-4010.	3.3	490
4	Wet but not slippery: boundary friction in tree frog adhesive toe pads. Journal of the Royal Society Interface, 2006, 3, 689-697.	1.5	323
5	Characterization of Photophysics and Mobility of Single Molecules in a Fluid Lipid Membrane. The Journal of Physical Chemistry, 1995, 99, 17662-17668.	2.9	254
6	Directional, passive liquid transport: the Texas horned lizard as a model for a biomimetic â€`liquid diode'. Journal of the Royal Society Interface, 2015, 12, 20150415.	1.5	168
7	Pemphigus foliaceus IgG causes dissociation of desmoglein 1–containing junctions without blocking desmoglein 1 transinteraction. Journal of Clinical Investigation, 2005, 115, 3157-3165.	3.9	152
8	Data analysis of interaction forces measured with the atomic force microscope. Ultramicroscopy, 2000, 82, 85-95.	0.8	148
9	Requirement of Rac activity for maintenance of capillary endothelial barrier properties. American Journal of Physiology - Heart and Circulatory Physiology, 2004, 286, H394-H401.	1.5	121
10	Moisture harvesting and water transport through specialized micro-structures on the integument of lizards. Beilstein Journal of Nanotechnology, 2011, 2, 204-214.	1.5	116
11	Morphometric characterisation of wing feathers of the barn owl Tyto alba pratincola and the pigeon Columba livia. Frontiers in Zoology, 2007, 4, 23.	0.9	110
12	A Nonparametric Test for the General Two-Sample Problem. Biometrics, 1998, 54, 1129.	0.8	105
13	Cadherin function probed by laser tweezer and single molecule fluorescence in vascular endothelial cells. Journal of Cell Science, 2003, 116, 1001-1011.	1.2	105
14	Ultrastructure and physical properties of an adhesive surface, the toe pad epithelium of the tree frog, <i>Litoria caerulea</i> White. Journal of Experimental Biology, 2009, 212, 155-162.	0.8	105
15	Slippery surfaces of pitcher plants: <i>Nepenthes</i> wax crystals minimize insect attachment <i>via</i> microscopic surface roughness. Journal of Experimental Biology, 2010, 213, 1115-1125.	0.8	101
16	Cuprizone treatment induces demyelination and astrocytosis in the mouse hippocampus. Journal of Neuroscience Research, 2009, 87, 1343-1355.	1.3	96
17	Cuprizone Treatment Induces Distinct Demyelination, Astrocytosis, and Microglia Cell Invasion or Proliferation in the Mouse Cerebellum. Cerebellum, 2009, 8, 163-174.	1.4	95
18	Biomechanics of ant adhesive pads: frictional forces are rate- and temperature-dependent. Journal of Experimental Biology, 2004, 207, 67-74.	0.8	92

#	Article	IF	CITATIONS
19	Intracellular Ca2+ Inhibits Smooth Muscle L-Type Ca2+ Channels by Activation of Protein Phosphatase Type 2B and by Direct Interaction with the Channel. Journal of General Physiology, 1997, 110, 503-513.	0.9	82
20	Flexural stiffness of feather shafts: geometry rules over material properties. Journal of Experimental Biology, 2012, 215, 405-415.	0.8	80
21	Accumulation and Distribution of Multiwalled Carbon Nanotubes in Zebrafish (<i>Danio rerio</i>). Environmental Science & Technology, 2014, 48, 12256-12264.	4.6	77
22	Cuprizone effect on myelination, astrogliosis and microglia attraction in the mouse basal ganglia. Brain Research, 2009, 1305, 137-149.	1.1	69
23	BLBP-expression in astrocytes during experimental demyelination and in human multiple sclerosis lesions. Brain, Behavior, and Immunity, 2011, 25, 1554-1568.	2.0	69
24	Mitochondrial Ca2+ mobilization is a key element in olfactory signaling. Nature Neuroscience, 2012, 15, 754-762.	7.1	64
25	Dynamic force microscopy imaging of native membranes. Ultramicroscopy, 2003, 97, 229-237.	0.8	62
26	The sandfish's skin: Morphology, chemistry and reconstruction. Journal of Bionic Engineering, 2007, 4, 1-9.	2.7	61
27	Micromechanics of smooth adhesive organs in stick insects: pads are mechanically anisotropic and softer towards the adhesive surface. Journal of Comparative Physiology A: Neuroethology, Sensory, Neural, and Behavioral Physiology, 2008, 194, 373-384.	0.7	59
28	Interactions of multiwalled carbon nanotubes with algal cells: Quantification of association, visualization of uptake, and measurement of alterations in the composition of cells. Environmental Pollution, 2015, 196, 431-439.	3.7	58
29	Ca2+Dependency of N-Cadherin Function Probed by Laser Tweezer and Atomic Force Microscopy. Journal of Neuroscience, 2003, 23, 11008-11014.	1.7	57
30	Bio-inspired microneedle design for efficient drug/vaccine coating. Biomedical Microdevices, 2020, 22, 8.	1.4	54
31	Investigating the Locomotion of the Sandfish in Desert Sand Using NMR-Imaging. PLoS ONE, 2008, 3, e3309.	1.1	53
32	Hydrothermal carbonization as an all-inclusive process for food-wasteÂconversion. Bioresource Technology Reports, 2018, 2, 77-83.	1.5	48
33	Two Closely Related Genes of Arabidopsis Encode Plastidial Cytidinediphosphate Diacylglycerol Synthases Essential for Photoautotrophic Growth. Plant Physiology, 2010, 153, 1372-1384.	2.3	47
34	Intracellular Ca2+ inactivates L-type Ca2+ channels with a Hill coefficient of approximately 1 and an inhibition constant of approximately 4 microM by reducing channel's open probability. Biophysical Journal, 1997, 73, 1857-1865.	0.2	46
35	Platelet-activating factor reduces endothelial nitric oxide production: role of acid sphingomyelinase. European Respiratory Journal, 2010, 36, 417-427.	3.1	46
36	Cell-Cell Contact Formation Governs Ca2+ Signaling by TRPC4 in the Vascular Endothelium. Journal of Biological Chemistry, 2010, 285, 4213-4223.	1.6	45

#	Article	IF	CITATIONS
37	A type 2A phosphatase-sensitive phosphorylation site controls modal gating of L-type Ca2+ channels in human vascular smooth-muscle cells. Biochemical Journal, 1996, 318, 513-517.	1.7	44
38	Neuronal cell growth on iridium oxide. Biomaterials, 2010, 31, 1055-1067.	5.7	44
39	The toxicity of silver nanoparticles to zebrafish embryos increases through sewage treatment processes. Ecotoxicology, 2013, 22, 1264-1277.	1.1	41
40	Two-Microelectrode Voltage Clamp of Xenopus Oocytes: Voltage Errors and Compensation for Local Current Flow. Biophysical Journal, 1999, 77, 1980-1991.	0.2	40
41	Affinity of Trans-interacting VE-cadherin Determined by Atomic Force Microscopy. Single Molecules, 2000, 1, 119-122.	1.7	38
42	Cribellate thread production in spiders: Complex processing of nano-fibres into a functional capture thread. Arthropod Structure and Development, 2015, 44, 568-573.	0.8	38
43	Role of transglutaminase�1 in stabilisation of intercellular junctions of the vascular endothelium. Histochemistry and Cell Biology, 2004, 122, 17-25.	0.8	37
44	VASP-dependent regulation of actin cytoskeleton rigidity, cell adhesion, and detachment. Histochemistry and Cell Biology, 2006, 125, 457-474.	0.8	36
45	Bio-inspired Microfluidic Devices for Passive, Directional Liquid Transport: Model-based Adaption for Different Materials. Procedia Engineering, 2015, 120, 106-111.	1.2	36
46	Intestinal LI-cadherin Acts as a Ca2+-dependent Adhesion Switch. Journal of Molecular Biology, 2007, 370, 220-230.	2.0	34
47	Possible roles of LI-Cadherin in the formation and maintenance of the intestinal epithelial barrier. Tissue Barriers, 2013, 1, e23815.	1.6	32
48	Extraplastidial cytidinediphosphate diacylglycerol synthase activity is required for vegetative development in <scp><i>Arabidopsis thaliana</i></scp> . Plant Journal, 2013, 75, 867-879.	2.8	32
49	Adhesion enhancement of cribellate capture threads by epicuticular waxes of the insect prey sheds new light on spider web evolution. Proceedings of the Royal Society B: Biological Sciences, 2017, 284, 20170363.	1.2	32
50	Endothelial barrier stabilization by a cyclic tandem peptide targeting VE-cadherin transinteraction in vitro and in vivo. Journal of Cell Science, 2009, 122, 1616-1625.	1.2	31
51	Trypsin increases availability and open probability of cardiac L-type Ca2+ channels without affecting inactivation induced by Ca2+. Biophysical Journal, 1995, 69, 1847-1857.	0.2	28
52	An Insulated Flexible Sensor for Stable Electromyography Detection: Application to Prosthesis Control. Sensors, 2019, 19, 961.	2.1	28
53	Imaging and Force Spectroscopy on Desmoglein 1 Using Atomic Force Microscopy Reveal Multivalent Ca2+-Dependent, Low-Affinity Trans-Interaction. Journal of Membrane Biology, 2007, 216, 83-92.	1.0	27
54	Boneâ€forming cells with pronounced spread into the third dimension in polymer scaffolds fabricated by twoâ€photon polymerization. Journal of Biomedical Materials Research - Part A, 2017, 105, 891-899.	2.1	26

#	Article	IF	CITATIONS
55	Heterotypic trans-Interaction of LI- and E-Cadherin and Their Localization in Plasmalemmal Microdomains. Journal of Molecular Biology, 2008, 378, 44-54.	2.0	25

 $_{56}$ Cutaneous water collection by a moisture-harvesting lizard, the thorny devil (<i>Moloch) Tj ETQq0 0 0 rgBT /Overlock 10 Tf $_{24}^{50}$ 702 Td (local content of the thorny devil (<i>Moloch) Tj ETQq0 0 0 rgBT /Overlock 10 Tf $_{24}^{50}$ 702 Td (local content of the thorny devil (<i>Moloch) Tj ETQq0 0 0 rgBT /Overlock 10 Tf $_{24}^{50}$ 702 Td (local content of the thorny devil (<i>Moloch) Tj ETQq0 0 0 rgBT /Overlock 10 Tf $_{24}^{50}$ 702 Td (local content of the thorny devil (<i>Moloch) Tj ETQq0 0 0 rgBT /Overlock 10 Tf $_{24}^{50}$ 702 Td (local content of the thorny devil (<i>Moloch) Tj ETQq0 0 0 rgBT /Overlock 10 Tf $_{24}^{50}$ 702 Td (local content of the thorny devil (<i>Moloch) Tj ETQq0 0 0 rgBT /Overlock 10 Tf $_{24}^{50}$ 702 Td (local content of the thorny devil (<i>Moloch) Tj ETQq0 0 0 rgBT /Overlock 10 Tf $_{24}^{50}$ 702 Td (local content of the thorny devil (<i>Moloch) Tj ETQq0 0 0 rgBT /Overlock 10 Tf $_{24}^{50}$ 702 Td (local content of the thorny devil (<i>Moloch) Tj ETQq0 0 0 rgBT /Overlock 10 Tf $_{24}^{50}$ 702 Td (local content of the thorny devil (<i>Moloch) Tj ETQq0 0 0 rgBT /Overlock 10 Tf $_{24}^{50}$ 702 Td (local content of the thorny devil (<i>Moloch) Tj ETQq0 0 0 rgBT /Overlock 10 Tf $_{24}^{50}$ 702 Td (local content of the thorny devil (<i>Moloch) Tj ETQq0 0 0 rgBT /Overlock 10 Tf $_{24}^{50}$ 702 Td (local content of the thorny devil (<i>Moloch) Tj ETQq0 0 0 rgBT /Overlock 10 Tf $_{24}^{50}$ 702 Td (local content of the thorny devil (<i>Moloch) Tj ETQq0 0 0 rgBT /Overlock 10 Tf $_{24}^{50}$ 702 Td (local content of the thorny devil (<i>Moloch) Tj ETQq0 0 0 rgBT /Overlock 10 Tf $_{24}^{50}$ 702 Td (local content of the thorny devil (<i>Moloch) Tj ETQq0 0 0 rgBT /Overlock 10 Tf $_{24}^{50}$ 702 Td (local content of the thorny devil (<i>Moloch) Tj ETQq0 0 0 rgBT /Overlock 10 Tf $_{24}^{50}$ 702 Td (local content of the thorny devil (<i>Moloch) Tj ETQq0 0 0 rgBT /Overlock 10 Tf $_{24}^{50}$ 702 Td (local content of the thorny devil (<i>Moloch) Tj ETQq0 0 0 rgBT /Overlock 10 Tf $_{24}^{50}$ 70

57	Bioinspired polymer microstructures for directional transport of oily liquids. Royal Society Open Science, 2017, 4, 160849.	1.1	23
58	Transmembrane cooperative linkage in cellular adhesion. European Journal of Cell Biology, 2002, 81, 161-168.	1.6	22
59	Mechanical activity and force-frequency relationship of isolated mouse papillary muscle: effects of extracellular calcium concentration, temperature and contraction type. Pflugers Archiv European Journal of Physiology, 2002, 445, 297-304.	1.3	21
60	"Fluidic diode―for passive unidirectional liquid transport bioinspired by the spermathecae of fleas. Journal of Bionic Engineering, 2018, 15, 42-56.	2.7	21
61	Short-Term Cuprizone Feeding Verifies N-Acetylaspartate Quantification as a Marker of Neurodegeneration. Journal of Molecular Neuroscience, 2015, 55, 733-748.	1.1	20
62	Different Ca2+ affinities and functional implications of the two synaptic adhesion molecules cadherin-11 and N-cadherin. Molecular and Cellular Neurosciences, 2008, 37, 548-558.	1.0	19
63	Ultra-Low-Power Digital Filtering for Insulated EMG Sensing. Sensors, 2019, 19, 959.	2.1	19
64	The external scent efferent system of selected European true bugs (Heteroptera): a biomimetic inspiration for passive, unidirectional fluid transport. Journal of the Royal Society Interface, 2018, 15, 20170975.	1.5	18
65	Estimating the number of channels in patch-clamp recordings: application to kinetic analysis of multichannel data from voltage-operated channels. Biophysical Journal, 1997, 72, 1143-1152.	0.2	17
66	Atomic Force Microscopyâ€Đerived Nanoscale Chip for the Detection of Human Pathogenic Viruses. Small, 2008, 4, 847-854.	5.2	17
67	Determination of the Young's modulus of the epicuticle of the smooth adhesive organs of <i>Carausius morosus</i> by tensile testing. Journal of Experimental Biology, 2014, 217, 3677-87.	0.8	17
68	Morphological adaptation of the calamistrum to the cribellate spinning process in Deinopoidae (Uloboridae, Deinopidae). Royal Society Open Science, 2016, 3, 150617.	1.1	17
69	Adsorption and movement of water by skin of the Australian thorny devil (Agamidae: <i>Moloch) Tj ETQq1 1 0.78</i>	4314 rgB⁻ 1.1	Г /Qyerlock
70	Modeling of Zinc Dynamics in the Synaptic Cleft: Implications for Cadherin Mediated Adhesion and Synaptic Plasticity. Frontiers in Molecular Neuroscience, 2018, 11, 306.	1.4	17
71	Laser-Based biomimetic functionalization of surfaces: from moisture harvesting lizards to specific fluid transport systems. International Journal of Design and Nature and Ecodynamics, 2014, 9, 206-215.	0.3	16
72	Plasmalemmal concentration and affinity of mouse vascular endothelial cadherin, VE-cadherin. European Biophysics Journal, 2002, 31, 532-538.	1.2	15

Werner Baumgartner

#	Article	IF	CITATIONS
73	Transglutaminase 1 Stabilizes β-Actin in Endothelial Cells Correlating with a Stabilization of Intercellular Junctions. Journal of Vascular Research, 2007, 44, 234-240.	0.6	15
74	N-cadherin-mediated cell adhesion is regulated by extracellular Zn ²⁺ . Metallomics, 2015, 7, 355-362.	1.0	15
75	Nanofibre production in spiders without electric charge. Journal of Experimental Biology, 2017, 220, 2243-2249.	0.8	15
76	Biomimetic Combs as Antiadhesive Tools to Manipulate Nanofibers. ACS Applied Nano Materials, 2020, 3, 3395-3401.	2.4	14
77	Comparative Investigations of the Sandfishs β-Keratin (Reptilia: Scincidae: <i>Scincus) Tj ETQq1 1 0.784314 Tissue Engineering, 0, 16, 1-9.</i>	rgBT /Ove 0.7	erlock 10 Tf. 13
78	Barn Owl Flight. Notes on Numerical Fluid Mechanics and Multidisciplinary Design, 2012, , 101-117.	0.2	13
79	Adaptation to life in aeolian sand: how the sandfish lizard, <i>Scincus scincus</i> , prevents sand particles from entering its lungs. Journal of Experimental Biology, 2016, 219, 3597-3604.	0.8	13
80	Comparative Investigations of the Sandfish's β-Keratin (Reptilia: Scincidae: <i>Scincus) Tj ETQq0 0 0 rgB and Tissue Engineering, 0, 15, 1-16.</i>	T /Overloc 0.7	k 10 Tf 50 4 12
81	Adaptive camouflage: What can be learned from the wetting behaviour of the tropical flatbugs <i>Dysodius lunatus</i> and <i>D. magnus</i> . Biology Open, 2017, 6, 1209-1218.	0.6	12
82	Beta-Actin is a Target for Transglutaminase Activity at Synaptic Endings in Chicken Telencephalic Cell Cultures. Journal of Molecular Neuroscience, 2012, 46, 410-419.	1.1	11
83	Capacitive Sensing of Surface EMG for Upper Limb Prostheses Control. Procedia Engineering, 2016, 168, 155-158.	1.2	11
84	Water transport through the intestinal epithelial barrier under different osmotic conditions is dependent on LI-cadherin trans-interaction. Tissue Barriers, 2017, 5, e1285390.	1.6	11
85	Basal dephosphorylation controls slow gating of L-type Ca2+ channels in human vascular smooth muscle. FEBS Letters, 1995, 373, 30-34.	1.3	10
86	Different pH-dependencies of the two synaptic adhesion molecules <i>N</i> -cadherin and cadherin-11 and the possible functional implication for long-term potentiation. Synapse, 2013, 67, 705-715.	0.6	10
87	Neutral glycans from sandfish skin can reduce friction of polymers. Journal of the Royal Society Interface, 2016, 13, 20160103.	1.5	10
88	Bio-inspired "fluidic diode―for large-area unidirectional passive water transport even against gravity. Sensors and Actuators A: Physical, 2018, 283, 375-385.	2.0	10
89	Impact of Femtosecond Laser Treatment Accompanied with Anodization of Titanium Alloy on Fibroblast Cell Growth. Physica Status Solidi (A) Applications and Materials Science, 2020, 217, 1900838.	0.8	10
90	Qualitative and Quantitative Characterisation of Major Elements in Particulate Matter from In-use Diesel Engine Passenger Vehicles by LIBS. Energies, 2020, 13, 368.	1.6	10

#	Article	IF	CITATIONS
91	Femtosecond Laser-Processing of Pre-Anodized Ti-Based Bone Implants for Cell-Repellent Functionalization. Nanomaterials, 2021, 11, 1342.	1.9	9
92	The function of 7D-cadherins: a mathematical model predicts physiological importance for water transport through simple epithelia. Theoretical Biology and Medical Modelling, 2011, 8, 18.	2.1	8
93	Sensory pits – Enigmatic sense organs of the nymphs of the planthopper Issus coleoptratus (Auchenorrhyncha, Fulgoromorpha). Arthropod Structure and Development, 2012, 41, 443-458.	0.8	8
94	Capacitively coupled EMG detection via ultra-low-power microcontroller STFT. , 2017, 2017, 410-413.		8
95	Repellent rings at titanium cylinders against overgrowth by fibroblasts. Advanced Optical Technologies, 2020, 9, 113-120.	0.9	8
96	Sandfish inspires engineering. , 2011, , .		7
97	Localization of VE-cadherin in plasmalemmal cholesterol rich microdomains and the effects of cholesterol depletion on VE-cadherin mediated cell–cell adhesion. Biochimica Et Biophysica Acta - Molecular and Cell Biology of Lipids, 2014, 1841, 1725-1732.	1.2	7
98	Signal evaluation of capacitive EMG for upper limb prostheses control using an ultra-low-power microcontroller. , 2016, , .		7
99	The Texas horned lizard as model for robust capillary structures for passive directional transport of cooling lubricants. Proceedings of SPIE, 2016, , .	0.8	7
100	A novel device for elimination of cancer cells from blood specimens. Scientific Reports, 2020, 10, 10181.	1.6	7
101	A Polydimethylsiloxane (PDMS) Waveguide Sensor that Mimics a Neuromast to Measure Fluid Flow Velocity. Sensors, 2019, 19, 925.	2.1	6
102	An expectation–maximisation algorithm for the deconvolution of the intrinsic distribution of single molecule's parameters. Computers & Chemistry, 2002, 26, 321-326.	1.2	5
103	Functionalization of Carbon Nanotubes. , 2012, , 911-919.		5
104	Electrodiffusion near an ion channel and the effect of mobile buffer. Computational Biology and Chemistry, 2004, 28, 67-73.	1.1	4
105	Simple Synthetic Jet Actuators for Cooling Applications Using Soft or Rigid Magnets. Procedia Engineering, 2016, 168, 1541-1546.	1.2	4
106	Major Chemical Elements in Soot and Particulate Matter Exhaust Emissions Generated from In-Use Diesel Engine Passenger Vehicles. , 2020, , .		4
107	An Optimised Surface Structure for Passive, Unidirectional Fluid Transport Bioinspired by True Bugs. Journal of Bionic Engineering, 2021, 18, 375-386.	2.7	4
108	Removing non-random artifacts from patch clamp traces. Journal of Neuroscience Methods, 1998, 82, 175-186.	1.3	3

#	Article	IF	CITATIONS
109	Functional morphology of the adhesive organs of stick insects (Carausius morosus). Proceedings of SPIE, 2011, , .	0.8	3
110	Finite Element Methods for Computational Nano-optics. , 2012, , 837-843.		3
111	The plant hopper <i>Issus coleoptratus</i> can detoxify phloem sap saponins including the degradation of the terpene core. Biology Open, 2016, 5, 252-255.	0.6	3
112	Friction-Reducing Sandfish Skin. , 2015, , 1-7.		3
113	Three-Dimensional Photonic Structures Fabricated by Two-Photon Polymerization for Microfluidics and Microneedles. , 2018, , .		2
114	Qualitative Characterisation of Trace Elements in Diesel Particulate Matter from In-Use Diesel Engine Passenger Vehicles by Means of Laser-Induced Breakdown Spectroscopy. , 0, , .		2
115	A Novel Screw Drive for Allogenic Headless Position Screws for Use in Osteosynthesis—A Finite-Element Analysis. Bioengineering, 2021, 8, 136.	1.6	2
116	Fullerenes for Drug Delivery. , 2012, , 898-911.		1
117	Three-dimensional photonic structures on transparent substrates fabricated by two-photon polymerization for use as cell substrates and for wetting experiments. , 2016, , .		1
118	Physiological relevance of epithelial geometry: New insights into the standing gradient model and the role of LI cadherin. PLoS ONE, 2018, 13, e0208791.	1.1	1
119	The sandfish lizard's aerodynamic filtering system. Bioinspiration and Biomimetics, 2020, 15, 036003.	1.5	1
120	Identification of the Minor Chemical Elements in the Particulate Matter Exhaust Emissions From In-Use Diesel Engine Passenger Vehicles. , 2020, , .		1
121	The Impact of a Flexible Stern on Canoe Boat Maneuverability and Speed. Biomimetics, 2020, 5, 7.	1.5	1
122	Steady-state gel electrophoresis of long polymer molecules: a theoretical study. European Biophysics Journal, 2000, 29, 61-65.	1.2	0
123	Wolfgang Bargmann-Preis 2006 Pemphigus foliaceus IgG causes dissociation of desmoglein 1-containing junctions without blocking desmoglein 1 transinteraction +. Annals of Anatomy, 2006, 188, 501-502.	1.0	0
124	Cellular Targeting And Function Of Trpc4 Channels In Human Vascular Endothelium. Biophysical Journal, 2009, 96, 264a.	0.2	0
125	Fundamental Properties of Zinc Oxide Nanowires. , 2012, , 919-927.		0
126	Polydimethylsiloxane (PDMS) Waveguide Sensor Detecting Fluid Flow Velocity by Mimicking the Fish Lateral Line Organ. Proceedings (mdpi), 2018, 2, 885.	0.2	0

#	Article	IF	CITATIONS
127	AMROBS: All-Metal Replicas of Biological Surfaces—A Novel Approach Combining Established Techniques. Biomimetics, 2018, 3, 31.	1.5	Ο
128	Knowledge Acquisition from a Biomechanical System: Human Gait Transition as an Example. British Biomedical Bulletin, 2018, 06, .	0.0	0
129	Quantification of Minor Chemical Elements in Particulate Matter Collected from In-Use Diesel Engine Passenger Vehicles by Laser-Induced Breakdown Spectroscopy. Energies, 2020, 13, 6113.	1.6	0
130	Friction-Reducing Sandfish Skin. , 2016, , 1261-1267.		0
131	Evaluation of Capacitive EMG Sensor Geometries by Simulation and Measurement. Mathematics in Industry, 2018, , 13-23.	0.1	0
132	Spectrochemical Analytical Characterisation of Particulate Matter Emissions Generated from In-Use Diesel Engine Vehicles. Environmental Sciences Proceedings, 2020, 4, .	0.3	0
133	Qualitative and quantitative characterisation of minor chemical elements in Diesel Particulate Matter by Laser Induced Breakdown Spectroscopy. , 2020, 67, .		Ο